The Structure of Polymeric Alkylpyridinium Monolayers Spread on Water Studied by Specular X-ray and Neutron Reflection

D. A. Styrkas and R. K. Thomas*

Physical Chemistry Laboratory, South Parks Road, Oxford OX1 3QZ, U.K.

Z. A. Adib, F. Davis, P. Hodge, and X. H. Liu

Department of Chemistry, University of Manchester, Oxford Road, Manchester M13 9PL, U.K.

Received April 4, 1994®

ABSTRACT: Grazing incidence X-ray reflection has been used to examine the structure of spread monolayers of poly(*N*-alkyl-4-vinylpyridinium bromide)s, denoted by PC_n where n is the length of the alkyl side chain, on water. Members of the series with even n from 8 to 22 were investigated, and the results for PC_{18} are compared with those of neutron reflection on the same sample. The comparison of neutron and X-ray results on PC_{18} makes it possible to identify those contributions to the X-ray reflectivity coming from the polymer backbone and alkyl chains for this particular polymer. On the basis of this comparison the thickness of the polymer layer has been estimated for each member of the series. The ratio of the observed thickness of the monolayer to its maximum possible value (δ/l) varies from 1.3 for n = 8 through a minimum of 0.7 at n = 16 to 0.8 at n = 22. Even when allowance is made for the contribution of capillary waves to the thickness of the layer, δ/l remains above unity for the shortest chain compounds. This is interpreted as arising from disorder in the layer. As the side chain length increases, it imposes order on the chain orientations. For small n an increase of n therefore decreases the thickness of the layer, but once the side chains are reasonably ordered the increase in chain length causes the thickness to increase once more. The X-ray reflectivity shows, independently of the neutron result, that part of the polymer layer protrudes out of the water. For small n this projection is about one-third of the thickness of the total monolayer thickness, but this proportion increases with n until eventually it has reached about half the total thickness of the layer. Comparison with similar dimensions in surfactant layers and the PC_n Langmuir–Blodgett films indicates similar behavior at small n. The comparison between LB films and the precursor monolayer of the PC_n shows that disorder in the latter carries over into the LB film.

Introduction

Monolayers of amphiphilic polymers at the air–water interface are of interest because such systems are some of the simplest involving polymers at interfaces and also because they may be the precursors to polymeric Langmuir–Blodgett (LB) films. LB films have numerous potential applications in micro- and opto-electronics.[1,2] This is particularly the case for polymeric LB films, as they are more robust than nonpolymeric films. One application is devices based on second harmonic generation (SHG). Films for such devices must be noncentrosymmetric and contain a highly polarizable π-electron system.[3] Several all-polymeric LB films for SHG have been described recently: see, for example, refs 4–6 and references cited therein. The nonsymmetric LB films used are generally Y-type films prepared from two different polymers deposited alternately. One polymeric amphiphile contains the "active" moiety; the other is a "passive" polymer. We recently showed that poly(*N*-docosyl-4-vinylpyridinium bromide) served as a particularly good passive polymer.[4] This is probably associated with the fact that this and some other polymers of the same general type form some of the best organized polymeric LB films so far investigated as judged by the number of Bragg peaks obtained in X-ray studies.[7]

In this paper we present the study of spread monolayers of poly(*N*-alkyl-4-vinylpyridinium bromide)s, denoted by PC_n, on water using specular X-ray and neutron reflection. The range of wavevectors accessible in neutron and X-ray reflection enables one to study layer thickness and structure on a molecular scale, and these techniques are therefore suitable for investigating the properties of monolayers deposited on the water surface.[8,9] The structural information obtained in such experiments is of particular importance for the deeper understanding of the structure of the monolayer presursors of the LB films.

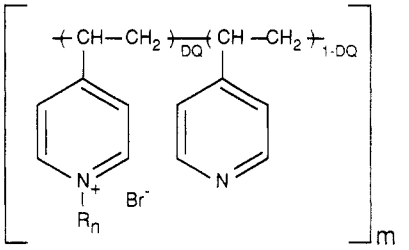

Figure 1. Structure of poly(*N*-alkyl-4-vinylpyridine) bromide compounds.

Experimental Details

The Teflon Langmuir trough had two moving barriers with a working area which could be varied between 200 and 70 cm^2. The surface pressure was controlled with ±1 mN/m accuracy using an induction sensor with spring and Wilhelmy plate. High purity water (Elga Ultrapure system) was used throughout as a subphase. The PC_n (see Figure 1) were synthesized by quaternization of poly(vinylpyridine) (M_v = 42 700, by viscometry in ethanol at 25 °C) as described previously.[7] The fraction of reacted pyridine moieties (degree of quaternization = DQ) for each compound is shown in Table 1. The deuterated polymer was prepared similarly and had a DQ of 0.85. PC_n solutions in chloroform (Aldrich, HPLC) of approximately 0.02 wt % concentration were used to deposit the monolayer on the water subphase. The X-ray measurements are very sensitive to vibration, and a vibration free table (Vibration Isolation System Mod-2, JRS) together with a heavy granite block was used to eliminate external vibrations of the surface. The granite block could be raised and lowered remotely, which made it possible to maintain the level of the

® Abstract published in *Advance ACS Abstracts*, August 1, 1994.

0024-9297/94/2227-5504$04.50/0 © 1994 American Chemical Society

Table 1. Parameters of the Poly(*N*-alkyl-4-vinylpyridines)

alkyl bromide $C_nH_{n+1}Br$ used to quaternize polymer, n	degree of quaternization ±0.07[7]	area per segment at π = 0 mN/m, Å^2	area per segment, Å^2	collapse pressure π_c, mN/m
8	1.00	40	30	26
10	0.95	42	33	45
12	0.90	36	29	30
14	0.90	41	31	33
16	0.41	50	41	40
18	1.00	48	36	38
20	1.00	43	35	50
22	1.00	46	36	42

water surface with an accuracy of 10 μm. The X-ray reflection measurements were made on a home-built X-ray reflectometer[10] using a conventional X-ray tube (Cu Kα, 1.54 Å). The dynamic range of the reflectometer is such that one can measure reflectivities from 1 down to 10^{-7}. The background scattering was determined by measuring the reflectivity at high values of the momentum transfer normal to the interface ($Q = 4\pi(\sin\theta)/\lambda$) and assuming it to be flat. Neutron reflection measurements were made on the reflectometer CRISP at ISIS using a procedure described previously.[11]

Results and Discussion

Monolayers on Pure Water. The pressure/area isotherms of the PC_n compounds have been presented in ref 7. Except for PC_8 the reflectivity measurements were made at a surface pressure of 30 mN m^{-1}, which is about two-thirds of the way up the knee of the isotherm. At this pressure the areas per segment through the series (see Table 1) fall into two groups, 38 ± 3 Å^2 for PC_n with n equal to 16 or more, and less than about 33 Å^2 when n is 14 or less.

The monolayers were conditioned in two different ways, by "slow" compression where the monolayer was allowed to settle for 15–20 min before compressing it to the required pressure and then either maintaining the surface pressure constant or using two successive compressions and expansions of the monolayer before the final compression, or by "quick" compression. In the quick method the monolayer was compressed over an interval of 5 min up to the required surface pressure immediately after spreading. No difference was found between reflectivity profiles of the monolayers prepared by these two means.

Figure 2 shows the reflectivity profiles of monolayers with the shortest (PC_8) and longest (PC_{22}) side chains. There is a marked break in the reflectivity of the monolayer of PC_{22} at a momentum transfer of about 0.2 Å^{-1}. This corresponds to the trough of an interference fringe resulting from part of the polymer layer protruding from the water, which can be understood as follows. The kinematic approximation for the reflectivity consists of two terms, a rapidly decaying part depending only on the difference between the mean scattering lengths of air and subphase, $\Delta\rho$, and an interference term which depends on the interfacial inhomogeneity.[12] The first term is

$$R(Q) = 16\pi^2\Delta\rho/Q^4 \quad (1)$$

For the especially simple case of a single uniform layer at the interface the second term is

$$Q^2h(Q) = \Delta\rho^2 - 4\rho_l(\Delta\rho - \rho_l)\sin^2(Qt/2) \quad (2)$$

where ρ_t is the scattering length density of the layer and t is its thickness. If ρ_l is less than $\Delta\rho$ the interference term initially depresses the reflectivity below its normal value and leads to a trough at π/t. Since, in the simple formulation of eq 2, the amplitude of the interference term depends on the value of ρ_t relative to $\Delta\rho$, we can

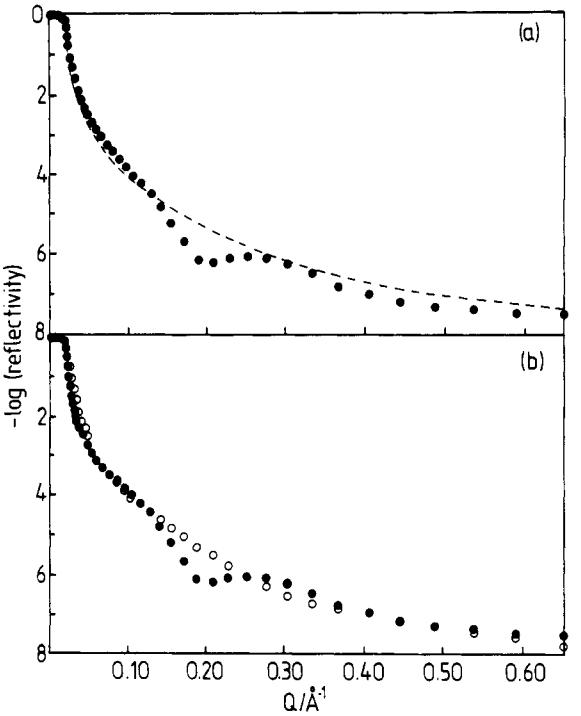

Figure 2. (a) X-ray reflectivity profiles from water (dashed line) and a PC_{22} monolayer spread on water at a surface of 30 mN m^{-1}. (b) X-ray reflectivity profiles for a spread PC_8 monolayer (O) compared with the profile of PC_{22} shown in (a).

immediately deduce that the layer causing the interference effect has a significantly lower scattering length density than the subphase. By fitting the depth and position of the break in the profile, we can also deduce an approximate value of ρ_t and the approximate thickness t of the layer.

The reflectivity profiles of the other PC_n with n = 10, 12, 14, 16, 18, and 20 fall between the two extreme cases of PC_{22} and PC_8, the break on each profile shifting to a higher momentum transfer and the amplitude of the trough decreasing, as the length of the hydrocarbon chain decreases (Figure 3). From the argument presented in the previous paragraph we can deduce from the break an estimate of the variation of thickness of the protruding region of the layer with n. This variation is shown in Figure 4. Apart from PC_{10} the thickness of the layer is seen to be approximately constant from n = 8 to 14 before rising steadily for polymers with the longer side chain length. This method of determining the thickness of the protruding layer is crude and a more detailed model of the layer does reduce the derived thickness (see below). However, the simple analysis does demonstrate that some structural information can be deduced directly and in a reasonably model independent manner.

When the reflectivity profiles are calculated exactly using the optical matrix method,[11] more accurate values can be deduced for the thickness and scattering length density of the protruding layer. From the fitted scattering length and the known average number of electrons per polymer segment the fraction of polymer in this protruding layer may be deduced from

$$\rho_l = \phi\rho/tA \quad (3)$$

where Φ is the fraction of polymer in the protruding layer and ρ is given by

$$\rho = \sum n_i f_i \frac{e^2}{mc^2} \quad (4)$$

where n_i and f_i are the number density and atomic

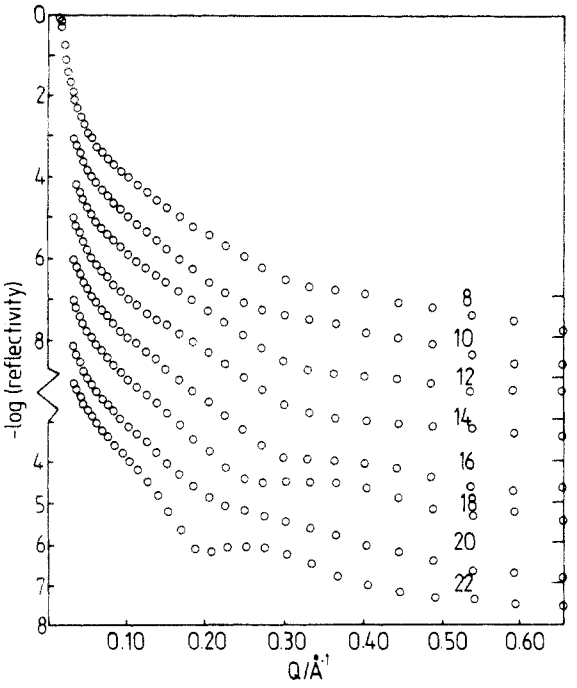

Figure 3. X-ray reflectivity profiles of spread monolayers of PC_n on water from $n = 8$ to $n = 22$. The vertical axes of the profiles are displaced, and the limiting values of reflectivities at high Q are marked. The size of the circles indicates the error bars.

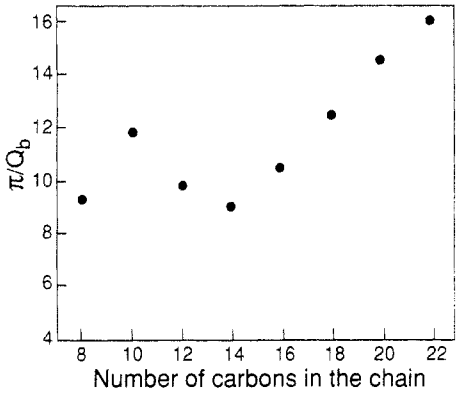

Figure 4. Variation of the apparent thickness of the protruding polymer layer as determined by π/Q_b, where Q_b is the position of the "break" in the reflectivity profile, with the number of carbon atoms in the polymer side chain.

scattering factor for atom i, e and m are the charge and mass of the electron, and c is the speed of light. For example for PC_{18} the thickness of this layer was found to be 12.5 Å and the optimum value of ρ_1 to be 6×10^{-6} Å^{-2} (see Figure 5). Given the known value of 36 Å^2 for the area per molecule from the π–A isotherm, 50% of the polymer is found to be out of the water. However, as can be seen from Figure 5, such a simple model of the layer does not account well for the observed reflectivity other than for the break. To improve the fit, we used a procedure illustrated with PC_{18} as an example.

There are two regions of the reflectivity profile in Figure 5 where the fit of the one layer model is poor. The calculated reflectivity is too low in the region of $Q \sim 0.1$ Å^{-1} and is too high in the region of $Q \sim 0.5$ Å^{-1}. The obvious next step is to constrain the stoichiometry of the system correctly and include the 50% of the polymer not accounted for by the single protruding layer model. There are essentially two ways of doing this reasonably directly, either as a second space filling layer or as a second space filling layer including water. Either way requires

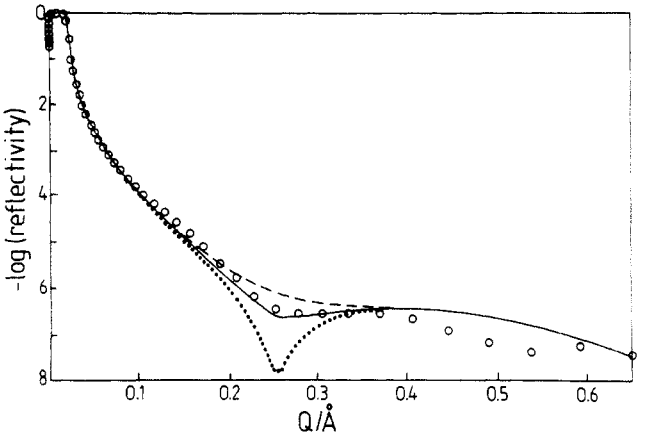

Figure 5. X-ray reflectivity profile for the PC_{18} monolayer on the water surface (O) and the fit using a single uniform monolayer of thickness 12.5 Å of scattering length density 7 (dashed line), 6 (continuous line), and 5×10^{-6} Å^{-2} (dotted line). The size of the circles indicates the error bars.

approximate values of the molar volume of the different fragments.

We take the following volumes for the component parts of the polymer: CH_2 group volume 27 Å^3,[14] vinylpyridine fragment volume 190 Å^3 (from the density of vinylpyridine), and bromide 30 Å^3. The scattering length density of the pure polymer is then estimated to be 10.5×10^{-6} and 8.4×10^{-6} Å^{-2} with and without Br^-, respectively. When the value of 8.4×10^{-6} Å^{-2} is compared with the value of 6×10^{-6} Å^{-2} for the protruding layer, it can be seen that the space available in the latter is only about 70% filled. The simpler of the two possible assumptions above is that the remaining 50% of the polymer forms a space filling layer underneath the "protruding" layer. With the parameters of the protruding layer as before, the calculated profiles with a second close-packed layer of polymer are compared with the observed data in Figure 6 as dotted and dashed lines for polymer with and without the Br^- ion, respectively. Neither profile accounts for the observed reflectivity in the region of $Q = 0.5$ Å^{-1}, but the inclusion of the bromide ion does account for the region around $Q = 0.1$ Å^{-1}. It is, however, physically implausible that the bromide ion and the charged fragments of the polymer would be in a layer containing no water, and the second possibility, that the second layer also contains water, is more realistic. Including some water in the second layer both changes its scattering length density and, because of a combination of the space filling and stoichiometry constraints, its thickness. When the volume of a water molecule is taken to be 30 Å^3, the scattering length density and thickness of the second layer are therefore completely determined by the 50% of polymer and the number of water molecules per polymer segment. The best fit was obtained with three molecules of water per segment and is shown as a continuous line in Figure 6. However, this still does not account well for the observed profile at the higher values of Q. The reflectivity at the higher values of Q is sensitive to the finer detail of the structure of the layer, and it is therefore probable that further division of the layer into its components is necessary to fit the experimental data. The most likely explanation is that this second space filling layer is split into at least two regions.

The charged fragments of the layer including the Br^- counterion are expected to be more hydrated than the uncharged parts of the polymer, some of which must be present in the second layer if this layer contains 50% of the polymer. It is therefore plausible to divide the second layer into regions 2 and 3, 2 being next to the outer polymer

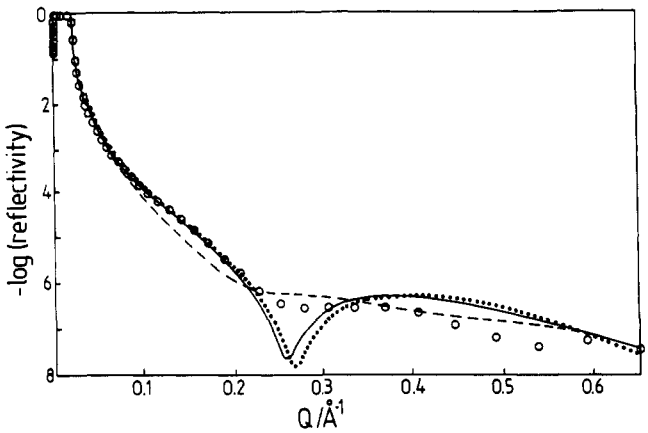

Figure 6. X-ray reflectivity profile for the PC_{18} monolayer on the water surface (O) and the fit using a stoichiometric two layer model of (i) the polymer without bromide ions (dashed line, layers 12.5 Å, 6×10^{-6} Å^{-2}, and 8 Å, 8.4×10^{-6} Å^{-2}), (ii) the polymer including bromide ions (dotted line, layers 12.5 Å, 6×10^{-6} Å^{-2}, and 8.7 Å, 10.5×10^{-6} Å^{-2}), and (iii) the polymer including bromide ions with the remaining space in layer 2 filled with water (continuous line, layers 12.5 Å, 6×10^{-6} Å^{-2}, and 11 Å, 10.3×10^{-6} Å^{-2}). The size of the circles indicate the error bars.

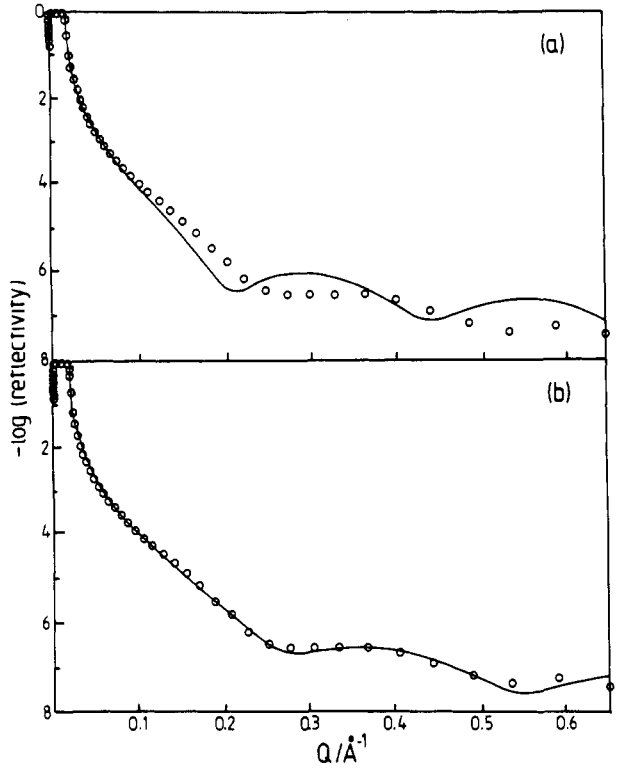

Figure 7. X-ray reflectivity profile for the PC_{18} monolayer on the water surface fitted with (a) a three layer model with layer 1 (12.5 Å, 6×10^{-6} Å^{-2}), layer 2 (10 Å, 8.6×10^{-6} Å^{-2}), and layer 3 (3 Å, 12.0×10^{-6} Å^{-2}) and (b) the four layer model with the parameters given in Table 2. The size of the circles indicates the error bars.

layer and containing most of the polymer, with some water as above, and layer 3 consisting mainly of water and bromide ions. When this was attempted, it was found that inclusion of the stoichiometric amount of Br^- in layer 3 caused the break at $Q \sim 0.2$ Å^{-1} to be too sharp. A better fit of the amplitude of the fringe was obtained if only half the bromide was included in this layer. Keeping the values for layer 1 and layer 2 as before, but with no Br^- in layer 2, the addition of the third layer had the effect shown in Figure 7a. It is immediately clear to anyone with experience of fitting reflectivity profiles that the amplitude of the interference features is well explained by this model, but that the thickness of the layers are too large. When

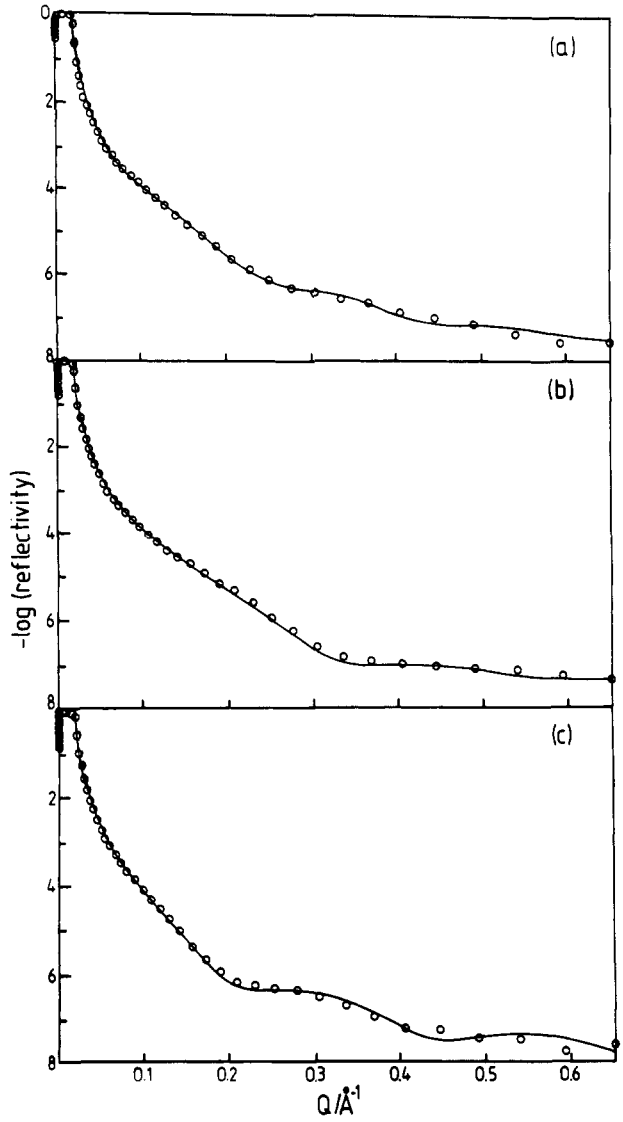

Figure 8. Observed and calculated X-ray reflectivity profiles (a) PC_{10}, (b) PC_{14}, and (c) PC_{22}. The continuous lines are calculated using the parameters given in Table 2. The size of the circles indicates the error bars.

Table 2. Parameters Used to Fit X-ray Reflectivity Profiles

	layer 1		layer 2		layer 3		layer 4	
alkyl chain	l, Å (±0.5)	$10^6\rho$, Å^{-2} (±0.2)	l, Å (±0.5)	$10^6\rho$, Å^{-2} (±0.3)	l, Å (±0.5)	$10^6\rho$, Å^{-2} (±0.1)	l, Å ±1	$10^6\rho$, Å^{-2} (±0.1)
8	7.0	6.0	8.0	8.5	5.0	10.0		
10	8.0	6.3	7.0	8.7	9.0	9.8	4	10
12	8.0	6.2	6.5	9.2	7.0	9.8		
14	8.0	6.1	6.5	9.0	3.0	9.8		
16	8.0	5.4	7.0	8.5	2.0	9.8	4	10
18	9.0	6.0	7.0	8.5	4.0	9.8	4	10
20	11.0	6.6	9.0	8.6	3.5	9.8	1	10
22	13.0	6.0	10.0	8.4	4.0	9.8	2	10

the thickness is diminished, while the stoichiometry and space filling are maintained, apart from the Br^- deficiency referred to above, a good fit to the observed data is obtained with the three layer model (Figure 7b). In the case of PC_{18} it is possible to include the full stoichiometric amount of bromide by adding a fourth diffuse layer. It is the parameters of this four layer structure that are given for all the PC_n in Table 2. However, the fit is not at all sensitive to this fourth layer and the only definite conclusion that may be drawn is that not all the bromide is strongly bound to the polymer.

The 3(4) layer model fits the whole set of data within error with the parameters given in Table 2, and Figure 8

shows fits of the model to PC_{10}, PC_{14}, and PC_{22}. A further refinement to the model would be to include roughness. The introduction of roughness at the outer surface has the general effect of reducing the reflectivity according to the equation

$$R(Q) = R_s(Q) \exp(-\sigma^2 Q^2) \quad (5)$$

where σ is the roughness. Roughness at the outer or inner interfaces of the layer will damp any interference effects but at any of the intermediate interfaces will mainly just damp interference effects from the layers concerned. For the PC_n a value of σ greater than about 3 Å (σ is 2.8 Å for pure water) causes the reflectivity to fall off more rapidly with Q than observed. It is similarly found that the introduction of roughness parameters greater than about 3 Å at the interfaces between layers 1 and 2 and between 2 and 3 makes it impossible to fit the data. Introduction of smaller values of σ at the different interfaces does have a small effect on the fitted parameters of the layers, but within the accuracy of the model, which has to be limited by the amount of chemical irregularity in the polymer structure, these differences are negligible.

Before any comprison of the structures of the layer with different chain lengths is made, it is worth considering the limitations of the model in more detail. The sensitivity of the profile to the model is high, and we are confident that the accuracy of the parameters in Table 2 is good. Ambiguities arise when one attempts to determine the proportions of polymer and water in layers 2 and 3. For X-rays there is little contrast between polymer and water. The only species in the solution that has a marked effect is the Br^- ion. Br^- cannot be in layer 2, because the scattering length density is too low, but is present in layer 3. In general, since the Br^- ion can be assumed to be close to the positive charge in the pyridinium group, it would seem that about half the pyridinium groups are in layer 3. However, because of the steric restraints acting on the polymer chain it is probable that there are also loops of polymer in this layer. It is not, however, possible to determine the fractionation of polymer between layers 2 and 3. For the short chain lengths not only is layer 3 significantly broad but the total volume of the polymer is too large to fit into layers 1 and 2. Thus in these cases polymer is definitely present in layer 3. We return to this question in the discussion section, after we have considered the neutron reflection results.

Neutron Reflection from PC_{18} Monolayers. As indicated above, X-rays cannot easily distinguish water and polymer and, consequently, the amount of polymer in layer 3 cannot be determined accurately from the X-ray measurement. The use of contrast variation in neutron reflection is more effective, although the resolution of the technique is not as good. Measurements were made of the reflectivity profiles of chain deuterated PC_{18} in null reflecting water and in D_2O and of the protonated PC_{18} in D_2O. The ratio of D_2O and H_2O in null reflecting water is such that its scattering length density is the same as that in air, and therefore it does not contribute at all to the reflectivity. Some care has to be taken in the interpretation of the set of profiles because the structures of the protonated and deuterated PC_{18} are not the same, as shown by differences in the X-ray profiles in Figure 9. The X-ray profile in the dPC_{18} was fitted as described in the previous section and found to differ mainly in layer 3 (see Table 3), which is broader than for hPC_{18}. Since there is a difference in the structure of layer 3 between the isotopes and the only thing that has changed is the polymer, this result already implies that there is a significant amount of polymer in layer 3.

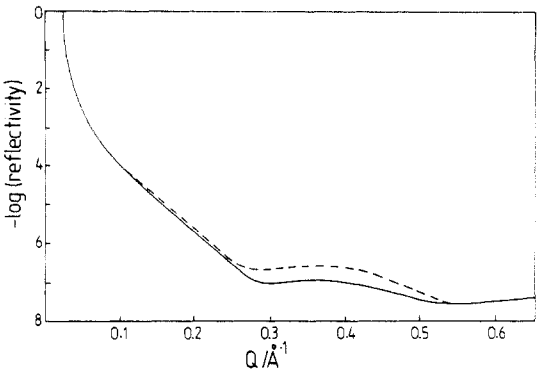

Figure 9. X-ray reflectivity profiles of fully protonated PC_{18} (dashed line) and side chain deuterated PC_{18} (continuous line). For clarity the best fitted lines have been shown rather than the experimental points.

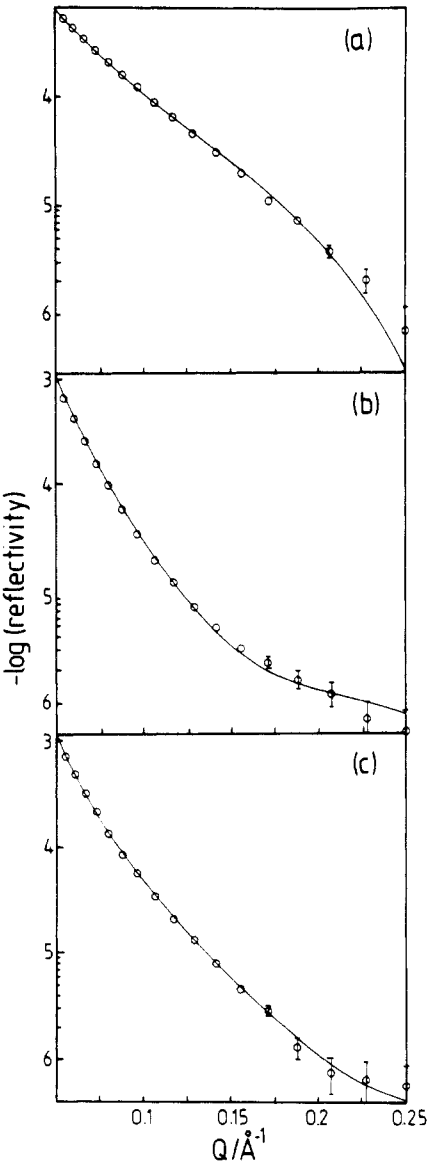

Figure 10. Neutron reflectivity profiles (a) deuterated PC_{18} on null reflecting water, (b) deuterated PC_{18} on D_2O, and (c) protonated PC_{18} on D_2O. The fitted lines are for the parameters given in Table 4.

The three neutron profiles are shown in Figure 10. Unlike the X-ray profiles these were only measured over a limited range of momentum transfer. However, it is the range over which the reflectivity is most sensitive to the structure of the layer. For hPC_{18} on D_2O the contrast is such that, to a good approximation, all that is observed is the region containing D_2O and this is found to be 14 Å

Table 3. Neutron and X-ray Results on PC_{18}

			Σ^l, Å
X-rays (dPC_{18})	8.5 Å, 5×10^{-6} Å^{-2}		22.5
	7 Å, 8.5×10^{-6} Å^{-2}	7 Å, 9.8×10^{-6} Å^{-2}	
dPC_{18}/D_2O	11 Å, 4.3×10^{-6} Å^{-2}	12 Å, 5.2×10^{-6} Å^{-2}	23
hPC_{18}/D_2O	10 Å, -0.03×10^{-6} Å^{-2}	13.5 Å, 1.63×10^{-6} Å^{-2}	23.5
dPC_{18}/NRW	11 Å, 4.27×10^{-6} Å^{-2}	12 Å, 4.6×10^{-6} Å^{-2}	23

thick and to be 30% water. For dPC_{18} on null reflecting water the only contribution to the neutron reflectivity is from the polymer. Taking the polymer layer to be uniform gives a mean thickness of 23 Å. Comparison of these two values with the X-ray results in Table 2 indicates that the polymer does indeed occupy layer 3 and may even extend into layer 4. Thus the total thickness of layers 2 and 3 in the X-ray fit, which should correspond to D_2O layer thickness of 14 Å, is 11 Å, and the total thickness of layers 1–3 is 22.5 Å, which corresponds closely with the 23 Å measured with neutrons. Confirmation of this structure is obtained by the fitting of a two layer model to the neutron data. Layer 1(N) is assumed to be entirely chains, and layer 2(N), to consist of the remainder of the polymer with solvent filling the empty space. This gives a good fit to the data for dPC_{18} (see continuous lines in Figure 10) with the first layer consisting of about 70% chains and 30% empty space and the second layer containing about 75% polymer and 25% water (the neutrons cannot distinguish bromide ions from water). A good fit was also obtained for the hPC_{18} with a first layer containing only chains, whose presence has a negligible effect on the reflectivity, and a second layer containing about 25% water. The parameters obtained from X-ray and neutron data on PC_{18} are summarized in Table 3.

Before discussing the significance of the geometrical parameters of the layer, we compare the results of the X-ray and neutron reflection measurements. Because of the selective effects of isotopic substitution on the neutron reflectivity there is no ambiguity about the interpretation of the neutron data, except insofar as there is a limit in the resolution of the experiment. Thus we can conclude that for PC_{18} the mean thickness of the polymer chain region is 23 Å, defined in terms of a uniform layer. X-ray reflection, on the other hand, does not distinguish polymer and subphase at all well, although it is clearly sensitive to the presence of the polymer layer. The interpretation is then much more model dependent than that of the neutron reflectivity. Nevertheless, we have shown that if full use is made of the available constraints, i.e. the known area per segment and stoichiometry, and if a range of similar compounds has been studied, it is possible to interpret the X-ray reflection quantitatively. However, without the neutron data, an important ambiguity would remain and that is how the polymer is distributed between layers 2 and 3, and possibly even 4. The importance of resolving this ambiguity is illustrated by the set of structural data for the layers, summarized in Table 4, which we now consider.

The 3(4) layer model of the structure modifies the conclusions drawn from the crude single layer model of a protruding polymer layer, which led to the plot shown in Figure 4. The thickness of this layer (layer 1) is reduced and varies slightly less erratically. Within error it is constant from n = 8 to 16 and then increases steadily. In the absence of the neutron data we would probably have interpreted the X-ray structure as consisting of the hydrophobic part of the polymer occupying layers 1 and 2 with the pyridinium fragments and bromide ions in layer 3. The combined thickness of layers 1 and 2 is given in column 3 of Table 4 and shows a variation parallel to that of layer 1, i.e. approximately constant for n = 8 to 16 and

Table 4. Comparison of Thickness Parameters for PC_n Monolayers, Langmuir–Blodgett Films, and C_nTAB Monolayers[a]

alkyl chain	layer 1 (Å)	layers 1 + 2, Å	total (δ) 1 + 2 + 3, Å	PC_n ratio δ/l	LB film ratio $\delta/2l$[7]	C_nTAB ratio δ/l[13]
8	7.0	15.0	20 (18.0)	1.3 (1.15)	1.04	
10	8.0	15.0	24 (22)	1.3 (1.20)	1.16	1.2 (1.00)
12	8.0	14.5	21.5 (19)	1.0 (0.90)	0.83	1.0 (0.85)
14	8.0	14.5	17.5 (14.5)	0.8 (0.65)	0.79	0.9 (0.80)
16	8.0	15.0	17 (14.0)	0.7 (0.55)	0.75	0.9 (0.80)
18	9.0	16.0	20 (17.5)	0.7 (0.60)	0.70	0.8 (0.75)
20	11.0	20.0	23.5 (21.5)	0.8 (0.70)	0.65	
22	13.0	23.0	27 (25.0)	0.8 (0.75)	0.61	

[a] Values in parentheses correspond to thicknesses corrected for capillary wave roughness as described in the text. The fully extended chain lengths, l, have been estimted from the values for the alkyl chains[12] plus 2.5 Å to allow for the head group in the C_nTABs and plus 4 Å for the PC_n.

increasing steadily at higher n. However, the neutrons show unequivocally that for PC_{18} the hydrophobic part of the polymer occupies layers 1, 2, *and* 3. We therefore assume that this is the case for *all* values of n. Then a quite different picture results. Column 4 of Table 4 gives this total thickness δ and shows that, apart from an abnormally large value of the thickness for PC_{10}, δ is large at small and large n, passing through a minimum at n = 14–16. This suggests that disorder of the layer contributes strongly to the thickness for small values of n and that as the side chains increase in length the monolayer becomes more and more ordered. This is confirmed by the following semiquantitative argument.

The polymer layer will have a thickness comparable with the fully extended chain if the chain is oriented vertically and if the incidence of gauche defects in the alkyl side chain is negligible. It can only be thicker than the fully extended chain length if there is significant surface roughness or disorder in the layer. We express the thickness of the layer as[15]

$$\delta^2 = \langle (l \cos\theta + d)^2 \rangle + w_s^2 + w_r^2 \qquad (6)$$

where $l \cos\theta$ is the projection of the chains along the surface normal, d is the intrinsic thickness of the remainder of the polymer, w_r is the capillary wave contribution to the roughness, and w_s accounts for any other roughness. Equation 6 is approximate in that there may be some coupling between the intrinsic dimensions of the polymer and the capillary waves, for example. Also, the division of the roughness into two is artificial but is done because it is possible to estimate the fraction arising from capillary waves with a simple model.[16] Strictly, δ and eq 6 refer to a Gaussian distribution but it is easy to make the extension to the uniform layers used here. A crude estimate of the contribution of the capillary waves to the roughness may be made by using the value for a pure liquid with the same surface tension. This may overestimate the roughness from this source because the polymer layer motions will be damped, but it is sufficient for our present purposes. When this correction is applied, we obtain the values of δ given in brackets in column 4 of Table 4. The PC_n with n of 8, 10, and 12 are still thicker than the fully extended, normally oriented, chains, those with n of 14, 16, and 18 are substantially thinner than the fully extended chains, but then there is a rapid increase in thickness for n = 20 and 22. The value of making this correction is that a better comparison can be made with the known values of the fully extended chain lengths. We make this comparison in column 5 of Table 4 in terms of the ratio of δ to the fully extended chain length, where once again the capillary wave

corrected values are given in brackets. Even after the removal of the capillary wave roughness the short side chain polymers form layers thicker than their fully extended dimensions.

A possible explanation for the changing relative thickness (δ/l) with n that it is associated with disorder in the orientation of the alkyl side chains. An explanation of this sort was originally given by Hodge et al.[17] who, on the basis of the pattern of the π–A isotherms of a series of styrene–maleic acid ester copolymers, suggested that short side chains point downward into the solvent and that long side chains initially point downward and then curl round the polymer backbone to finish in the lipophilic region of the monolayer. This model would cause δ/l to be unusually small for those chain lengths where the alkyl chain was partially curled round the backbone, and where the chain was pointing downward, δ/l would be normal. Although the relative chain does pass through a minimum at about PC_{18}, which would be consistent with this model, the model is not consistent with the large values of δ/l for PC_8 and PC_{10}. However, a more disordered version of this model would be that the short chain orientations are relatively random, with some pointing down into the solution, and that this randomness is gradually lost as the hydrophobicity of the chain increases with n and forces the chains to point more and more toward the lipophilic region, i.e. toward the air side of the interface. That the relative chain thickness remains below unity, even for PC_{22}, further suggests that, even when the chains are reasonably ordered, they are tilted significantly away from the surface normal. This model of orientational order increasing with n has also been observed in the series of surfactants, C_nTAB for which δ/l is given in column 7 of Table 4. For these surfactants there is direct evidence that the chains are tilted substantially away from the surface normal for n = 16[18] and that, even after subtraction of a capillary wave contribution, the layer is rough. We do not have the experimental information to make a separation of the angle of tilt and "excess" roughness for the PC_n series, but since it is unlikely that the only source of roughness is the capillary waves, we can use the values of δ/l to estimate the minimum value of the tilt angle of the chains away from the surface normal. We use the following simple model.

Although the chains in the longer chain compounds may be tilted at a relatively constant angle, we assume that that there is a distribution in the tilt angles of the shorter chains. We also assume that the width of this distribution has a much greater effect on the thickness of the layer than any occurrence of gauche defects in the alkyl side chains. The value of $\langle l \cos\theta + d\rangle^2$ in eq 6 can then be obtained by taking l to be the fully extended length of the side chain and averaging over a suitable distribution function for θ. A simple form of orientational distribution is

$$f(\theta,\varphi) = \cos^j\theta \tag{7}$$

which becomes increasingly peaked about $\theta = 0$ as j increases. It is assumed that the φ distribution is even. The thickness of the layer is obtained by substituting the expression for $f(\theta,\varphi)$ into

$$\delta^2 = \frac{l^2 \int d\varphi \int f(\theta) \cos^2\theta \sin\theta \, d\theta}{\int d\varphi \int f(\theta) \sin\theta \, d\theta} \tag{8}$$

If the integration of (8) is carried out over a solid angle only between $\theta = 0$ and $\pi/2$, i.e., the chains cannot have any orientation below the horizontal, then the value of δ/l varies with j according to

$$\delta/l = \left[\frac{j+1}{j+3}\right]^{1/2} \tag{9}$$

Thus the relative width of the polymer layer is less than unity unless j is large, i.e. unless the chains are highly oriented. If the distribution (7) is centered around a non-zero tilt angle, δ/l will remain less than unity even when the chains are all oriented in the same direction. The increase in δ/l from PC_{16} to PC_{22} may then be caused either by the angular distribution of the chains becoming more sharply peaked, i.e. j increasing, or by a decrease in the tilt angle. It is reasonable to suppose that for the lower members of the series the chain orientations must be more disordered. This has the effect of decreasing δ/l. The only way that values of δ/l greater than unity can then be explained is either because the chains are now free to take up all orientations from 0 to π or because the polymer backbone is increasingly disordered.

Since the spread monolayer is the precursor to Langmuir–Blodgett film formation, it would be expected that the disorder in the monolayer should be manifested in the LB film. Column 6 of Table 4 gives values of the relative thickness of a molecule assuming that one molecule has a thickness of half the periodic spacing in the LB film. As for the spread monolayer the two shortest chain polymers are both thicker than their fully extended lengths. This implies that the corresponding LB films are also significantly disordered. The decreasing value of δ/l with n suggests that the LB films become increasingly ordered with n and possibly that some interdigitation of the chains also occurs at high n. A further indication of the increasing order with n is that diffraction peaks out to third order were observed for PC_{18}, PC_{20}, and PC_{22}.[7]

Acknowledgment. D.A.S. thanks ICI plc for a scholarship. We also thank SERC Polymer and Composites Committee for their support for Z.A.A. and F.D.

References and Notes

(1) Vincett, P. S.; Roberts, G. G. *Thin Solid Films* **1980**, *68*, 135.
(2) Roberts, G. G. *Adv. Phys.* **1985**, *34*, 475.
(3) Embs, F.; et al. *Adv. Mater.* **1991**, *3*, 25.
(4) Hodge, P.; Ali-Adib, Z.; West, D.; King, T. A. *Thin Solid Films*, in press.
(5) Conroy, M.; Ali-Adib, Z.; Hodge, P.; West, D.; King, T. *J. Mater. Chem.* **1994**, *4*, 1.
(6) Hodge, P.; Ali-Adib, Z.; West, D.; King, T. *Macromolecules* **1993**, *26*, 1789.
(7) Davis, F.; Hodge, P.; Xiao-Hua, L.; Ali-Adib, Z. *Macromolecules*, in press.
(8) Penfold, J.; Thomas, R. K. *J. Phys. Condens. Matter* **1990**, *2*, 1369.
(9) Als-Nielsen, J. A.; Mohwald, H. *Handbook of Synchrotron Radiation*; North Holland: Amsterdam, 1992; Vol. 4.
(10) Bowler, R.; Lee, E. M.; Lee, S. K.; Styrkas, D. A.; Thomas, R. K. Manuscript in preparation.
(11) Lee, E. M.; Thomas, R. K.; Penfold, J.; Ward, R. C. *J. Phys. Chem.* **1989**, *93*, 381.
(12) Lu, J. R.; Simister, E. A.; Lee, E. M.; Thomas, R. K.; Rennie, A. R.; Penfold, J. *Langmuir* **1992**, *8*, 1837.
(13) Born, M.; Wolf, E. *Principles of Optics*; Pergamon Press: Oxford, U.K., 1990.
(14) Tanford, C. J. *J. Phys. Chem.* **1972**, *76*, 3020.
(15) Lu, J. R.; Simister, E. A.; Thomas, R. K.; Penfold, J. *J. Phys. Condens. Matter*, in press.
(16) Schlossman, M. L.; Schwartz, D. K.; Kawamoto, E. H.; Kellogg, G. J.; Pershan, P. S.; Kim, M. W.; Chung, T. C. *J. Phys. Chem.* **1991**, *95*, 6628.
(17) Hodge, P.; Khoshdel, E.; Tredgold, R. H.; Vickers, A. J.; Winter, C. S. *Br. Polym. J.* **1985**, *17*, 368.
(18) Lu, J. R.; Hromadova, M.; Thomas, R. K.; Penfold, J. *J. Phys. Chem.*, in press.